ACOUSTICS 2012

TLM OpenCL multi-GPUs implementation

G. Guillaume, N. Fortin, B. Gauvreau and J. Picaut

Département Infrastructures et Mobilité (IFSTTAR/IM), Route de Bouaye, CS4, 44344 Bouguenais Cedex
gwenael.guillaume@ifsttar.fr

Time-domain methods attracts much attention since a few years due to their ability to describe sound propagation in complex environments. However, such approaches requires a substantial computational power and a supercomputer remains still relevant for sound propagation simulations in huge domains. Graphics processing units (GPUs) are massively parallel computing environments, that are more and more used for scientific computations purposes. Among time-domain methods, the transmission line modeling (TLM) method is especially well adapted to this kind of hardware architecture. The paper presents an OpenCL™ implementation of the TLM method, this language being compatible with a wide range of available computational hardware, either with Central Processing Units (CPUs) or with GPUs devices. The algorithm is applied to evaluate the impact of various scenarios of vegetation cover on urban frontages and building rooftops within the framework of the VegDUD french project.

1 Introduction

Regarding environmental acoustics, the power increase of computing resources allows to consider more and more heavy numerical methods. Yet, the computational burden leads to make use of supercomputers [1], especially when considering huge propagation domains [2, 3]. Usually, the central processing unit (CPU) carries out all the instructions of computer programs. In parallel with multi-cores CPUs development, computational accelerators have been designed in order to handle multiple tasks simultaneously as parallel threads. Among these, the Graphics Processing Units (GPUs) show significant performances advancements. The raw computational power of a GPU widely surpasses the one of the most powerful CPU, and the gap is steadily widening [4]. GPUs potentialities were first highlighted through hardware acceleration in rasterization algorithmic tasks. However, the General Purpose computing on GPUs (GPGPU) also attracts a lot of attention in non-graphics fields, in particular in the scientific computation domain. Thus, in acoustics, this has been applied for many numerical methods as ray tracing technique [5], Finite Element Method (FEM) [6] or Boundary Element Method (BEM) [7], for Finite-Difference in the Time-Domain models [8], for the Lattice Boltzmann method [9, 10] and for solving the acoustic wave equation with Adaptive Rectangular Decomposition (ARD) technique [11]. The TLM method is also well suited for parallel distribution [12] and recent developments in electromagnetism has dealt with the parallization of the TLM algorithm on GPUs [13].

An OpenCL implementation of the TLM model has been performed within the framework of the VegDUD french project from the national research agency (ANR). This project involves lots of disciplinaries (acoustics, meterolorology, thermics, hydrologics, ...) in order to study the role of vegetation in urban sustainable development. Concerning acoustics, the objective is to observe and to analyze the effect of green covers on soundscape indicators as sound pressure level (SPL) or reverberation time (RT). The study is carried out by modelling sound propagation in a canyon street for which a few scenarios are evaluated, each scenario consisting in a particular configuration of building facades and/or rooftops covering.

The paper presents recent developments of the TLM method designed for outdoor sound propagation modelling. First, the TLM method is presented and its implementation is described by highlighting relevant tools specifically developed which allow complex shapes scenes voxelization as well as the modelling of huge propagation domain. Then, an application of the TLM model for evaluating various scenarios of vegetation covers is proposed and a few preliminary results are exposed and analyzed.

2 TLM method

2.1 TLM modelling

The TLM method is based on the Huygens' principle which states that a wavefront consists in a set of secondary sources radiating spherical wavelets whose envelopes can be broken down again into a new generation of secondary sources as well. This statement allows to describe sound propagation both through a spatial and a temporal discretization of the medium and of the propagation phenomena. This concept is numerically conveyed by replacing the propagation medium with a transmission lines network in which sound propagates in the form of sound pulses. Thereby, each junction, or node, links $N = 4$ or $N = 6$ transmission lines each other in two dimensions (2D) or three dimensions (3D) respectively, each transmission line being characterized by an impedance Z. Thereafter, the number of dimensions is called d such as d=2 and d=3 for creating a 2D and a 3D model respectively. Thus incident and scattered pulses are considered at each transmission lines junction and time increment. The propagation medium is discretized by means of an uniform cartesian meshing of mesh size $(\Delta l)^d$, Δl being the spatial step such as:

$$\Delta l \leqslant \frac{\lambda\sqrt{d}}{10}, \tag{1}$$

with λ the minimal wavelength of the simulation.

The scattered pulses at time increment t and node of discrete coordinates $\mathbf{r}$ such as

$$\mathbf{r} = \begin{cases} (i,j) & \text{for } d = 2 \text{ (\textit{i.e.} in 2D)}, \\ (i,j,k) & \text{for } d = 3 \text{ (\textit{i.e.} in 3D)}, \end{cases} \tag{2}$$

are related with the incident pulses to this node at the same time iteration by the following matrix relation:

$${}_t\mathbf{S_r} = \mathbf{D} \times {}_t\mathbf{I_r}. \tag{3}$$

where ${}_t\mathbf{I_r}$ and ${}_t\mathbf{S_r}$ are the vectors composed of the incident pulses ${}_tI^n_\mathbf{r}$ and of the scattered pulses ${}_tS^n_\mathbf{r}$ through each transmission line n (n = 1 to 6) respectively, $\mathbf{D}$ is a N by N scattering matrix given in the case of a 3D homogeneous propagation medium by:

$$\mathbf{D} = \frac{1}{d}\begin{bmatrix} 1-d & 1 & 1 & . \\ 1 & 1-d & 1 & . \\ 1 & 1 & 1-d & . \\ . & . & . & . \\ 1 & 1 & 1 & 1-d \end{bmatrix}. \tag{4}$$

The nodal pressure is written as a combination of all incident pulses, that is:

$${}_tp_\mathbf{r} = \frac{1}{d}\sum_{n=1}^{N} {}_tI^n_\mathbf{r}. \tag{5}$$

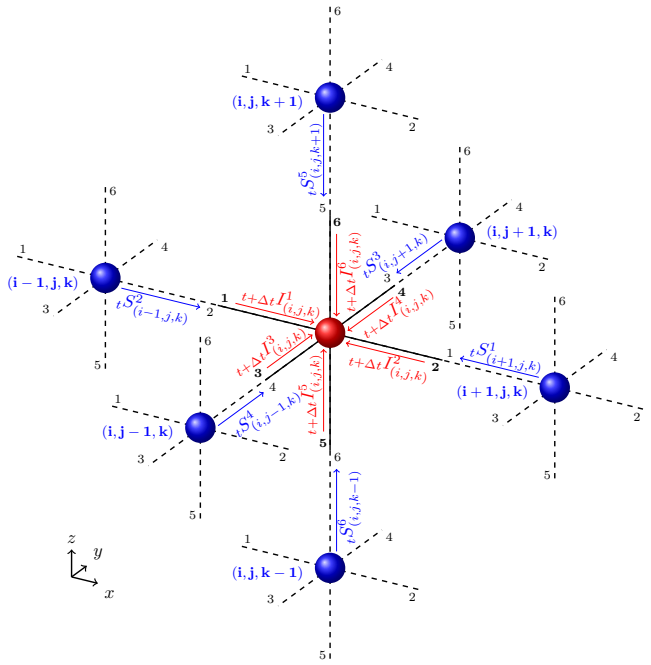

Figure 1: Representation of connexion laws in 3D.

In addition, the scattered pulses from neighbor nodes to node (i, j, k) at time increment t become the incident pulses to this node at the next time iteration $t+\Delta t$, Δt representing the time step defined by:

$$\Delta t = \frac{\Delta l}{\sqrt{d}\, c_0}, \tag{6}$$

with c_0 the sound speed in the propagation domain. This diffusion process is governed by connexion laws such as (Fig. 1):

$$_{t+\Delta t}I^n_{\mathbf{r}} = {}_tS^m_{\mathbf{r}^\pm_n}, \tag{7}$$

with

$$\left\{ \begin{array}{c} n \\ \mathbf{r}^\pm_n \end{array} \right\} = \left\{ \begin{array}{l} \left\{ \begin{array}{c} m-1 \\ \mathbf{r}^- \end{array} \right\} \quad \text{if } m \text{ is even,} \\ \left\{ \begin{array}{c} m+1 \\ \mathbf{r}^+ \end{array} \right\} \quad \text{if } m \text{ is odd,} \end{array} \right. \tag{8}$$

and

$$\mathbf{r}^\pm_n = \left\{ \begin{array}{l} (i \pm 1, j, k)\,, \text{ for } n = 1 \text{ or } 2, \\ (i, j \pm 1, k)\,, \text{ for } n = 3 \text{ or } 4, \\ (i, j, k \pm 1)\,, \text{ for } n = 5 \text{ or } 6. \end{array} \right. \tag{9}$$

See Refs. [14, 15] for details on the modelling of a dissipative and inhomogeneous propagation medium.

Boundaries are implemented in the TLM model at a distance $\Delta l/2$ from the nearest node in order to ensure the synchronism of sound pulses. They can be characterized by a reflection coefficient in pressure. The implementation of this kind of boundary condition is performed by modifying the connexion law for the nodes located near the reflecting boundary in the corresponding transmission line n as:

$$_{t+\Delta t}I^n_{\mathbf{r}} = R_n \cdot {}_tS^n_{\mathbf{r}}, \tag{10}$$

where R_n represents the boundary reflection coefficient in pressure. Complex impedance boundaries conditions can also be introduced in the TLM model [16]. The Miki impedance model [17] can be formulated as[18]:

$$Z(\omega) = Z_0 \left[1 + \frac{\varsigma}{(-j\omega)^{-\beta}} \right], \tag{11}$$

where

$$\varsigma = \frac{\alpha}{(2\pi\sigma)^\beta} \left[\sin\left(\frac{(\beta+1)\,\pi}{2} \right) \right]^{-1}, \tag{12}$$

σ is the specific airflow resistivity, and α=5.50 and β=−0.632. The impedance model is written as a partial fraction expansion which is formulated for the Miki model as follows [18]:

$$Z(\omega) = Z_0 \left[1 + \frac{\varsigma}{\Gamma(-\beta)} \sum_{k=1}^{K} \frac{a_k}{\gamma_k - j\omega} \right], \tag{13}$$

where Γ is Euler's gamma function, a_k and γ_k refer to the residuals and the real poles ($\gamma_k \geqslant 0$) of the partial fraction expansion respectively. These terms a_k and γ_k are computed through a minimization process of the root mean square error between Eqs. 11 and 13.

A virtual node is introduced outside the domain of interest and at a distance $\Delta l/2$ from the boundary. In the case of a boundary located at mid-distance between a virtual node $\mathbf{r}_v$ and a node $\mathbf{r}$, the scattered pulse from this virtual node is given by [16]:

$$\begin{aligned} {}_tS^n_{\mathbf{r}_v} = {}_tS^m_{\mathbf{r}} \left[\frac{-1+\Lambda_k}{1+\Lambda_k} \right] \\ + \frac{Z_0}{1+\Lambda_k} \sum_{k=1}^{K} \frac{a_k\, \varsigma}{\Gamma(-\beta)} \exp^{-\lambda_k \Delta t}\, {}_{t-\Delta t}\psi_{k_{\mathbf{r}}}, \end{aligned} \tag{14}$$

where

$$\Lambda_k = \frac{1}{\sqrt{d}} \left(1 + \sum_{k=1}^{K} \frac{a_k\, \varsigma}{\Gamma(-\beta)} \frac{1 - \exp^{-\lambda_k \Delta t}}{\lambda_k} \right). \tag{15}$$

In Eq. 14, the pressure pulse scattered by the virtual node at time t is a function of the recursive ψ_k function at the previous time increment $t - \Delta t$:

$$\begin{aligned} {}_{t-\Delta t}\psi_{k_{\mathbf{r}}} = \left(\frac{{}_{t-\Delta t}S^n_{\mathbf{r}} - {}_{t-\Delta t}S^m_{\mathbf{r}_v}}{\sqrt{d}\, Z_0} \right) \times \left(\frac{1 - \exp^{-\lambda_k \Delta t}}{\lambda_k} \right) \\ + \exp^{-\lambda_k \Delta t}\, {}_{t-2\Delta t}\psi_{k_{\mathbf{r}}}. \end{aligned} \tag{16}$$

Outdoor sound propagation modelling also requires to model open boundaries. Absorbing layers are modelled by weighting the connexion law (Eqs. 7) for the transmission line turned toward the computational domain limit by an attenuation factor $F_{\mathbf{r}}$ defined by [19]:

$$F_{\mathbf{r}} = (1+\epsilon) - \exp\left[\frac{-d^2_{\mathbf{r}}}{B} \right], \tag{17}$$

with $d_{\mathbf{r}}$ the distance from the computational domain limit, $0 < \epsilon \leqslant 1$ and where the decay constant B is given by:

$$B = -\frac{e^2_{AL}}{\ln \epsilon}. \tag{18}$$

The layer thickness e_{AL} can be expressed in term of number of nodes as:

$$e_{AL} = \frac{\lambda N_{\lambda_{AL}}}{\Delta l}, \tag{19}$$

where the parameter $N_{\lambda_{AL}}$ represents the equivalent depth of the absorbing layer in wavelength unit λ.

2.2 TLM algorithm

2.2.1 Heterogeneous platforms programming language

In 2008, the Khronos Group published the specification of OpenCL 1.0. This framework allows to write a code compatible with all operating systems and with all future devices (*e.g.* AMD®, Intel®, IBM®, NVidia®) without modification. Another main advantage of this programming environment is the generation and the dynamic built of source code to match with specified parameters. Providing source code during execution allows a speed-up gain by removing the source code corresponding to optional features like 2D code generation, meteorological effects consideration or source arrays introduction.

The TLM method requires several processing algorithm before and after the call of OpenCL computation core. This approach intensively uses matrix processing and calls third-party software like voxelization algorithm. Juggling simultaneously with all these libraries needs many sophisticated algorithms. Python open programming language was built for this purpose and a library called PyOpenCL is available to call OpenCL from Python.

2.2.2 Huge domain tuned algorithm

The TLM model is based on a regular meshing discretization of the propagation domain. A voxelization algorithm[1] has been designed in order to translate automatically a surfaces display (*i.e.* a polygon mesh) generated thanks to a computer-aided design (CAD) software into volumetric informations (*i.e.* a lattice of voxels). Moreover, in order to minimize the memory space required for huge computational domains while facilitating the identification of the sound propagation volumes, the consecutive identical elements of the matrix are merged according to one matrix dimension, the others dimensions being stored like a standard matrix.

In addition, a subdivision algorithm has been recently designed for splitting the computational domain in order to run high memory consuming simulations on a personal computer (Fig. 2). The huge domain is first splitted into blocks according to the available GPU memory. Then each block is enlarged with a buffer made with neighbor blocks parts such as the number M of cells inside the buffer in each cartesian direction determines the number of feasible time iterations calculations Δt inside the block. Thus data transfer frequency between GPUs and CPU is reduced. Thereafter, the unit time range UT represents the unit time for blocks computations such as $UT = M\Delta t$. Once the blocks are created, TLM calculations are performed as depicted at Fig. 3. At the end of each unit time range UT_i, buffers are updated with the data of the neighbors blocks. According to the required memory space, blocks data are stored at each time range UT_i.

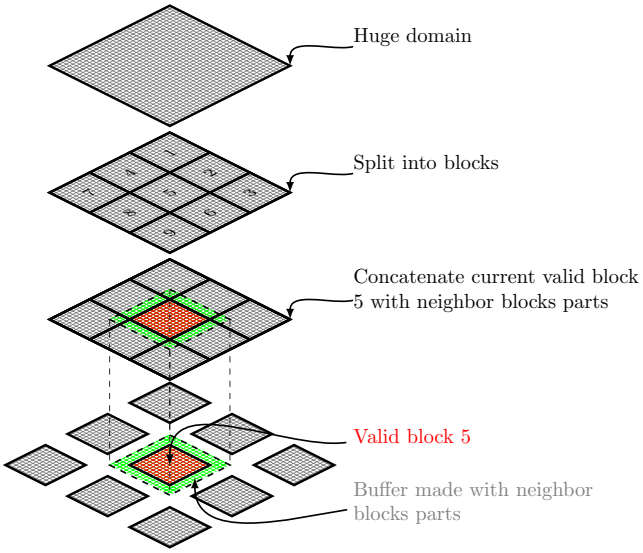

Figure 2: Blocks splitting process.

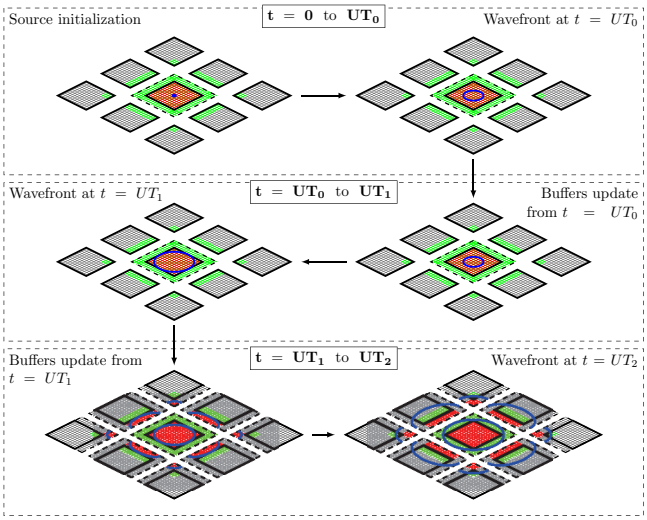

Figure 3: Blocks propagation.

3 Green covers study

3.1 Computational domain

The proposed TLM model is used for evaluating the role of vegetation cover in urban soundscapes. The computational domain is a canyon street as illustrated at Fig. 4. A two-way street passes between two identical buildings, each one being made up of four floors. A sidewalk and an off-street parking of 2 m width separate the two trafic lanes from the buildings facades.

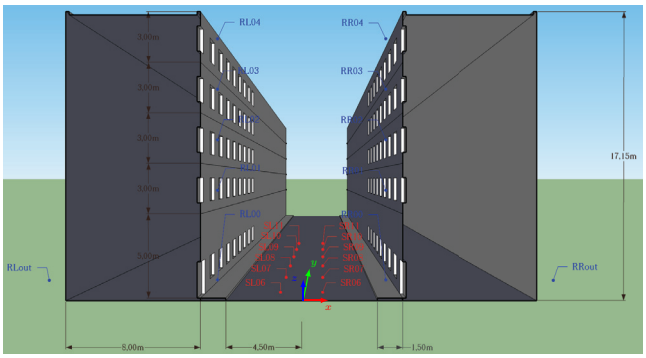

Figure 4: Sources and microphones locations in the canyon street. The line sources continue upstream from this view of the middle cross-section of the street.

Two-line sources, each composed of 11 omnidirectional

[1] https://github.com/nicolas-f/FastVoxel

point sources are located at 0.5 m high in the center of each trafic lane (*i.e.* at 1.25 m from the street longitudinal axis) all 5 m (Fig. 4 and Table 1) thanks to the I-simpa software[2]. The sources generate singly a gaussian pulse in order to create an incoherent excitation. This is produced by starting randomly the sources ones after the others. Ten microphones are positioned in the middle cross-section, each one at 1 m from a facade (Fig. 4 and Table 1). In the street, microphones face the center of an opening (a door or a window). Outside of the street, the microphones are located at 1.2 m high and at 1 m from the facade.

Table 1: Sources (S) and receivers (R) locations. The sign of x positions depend on the side location in the street: It is negative for left-side sensors and positive for right-side ones.

	S01	S02	S03	S04	S05	S06
x (m)	±1.25	±1.25	±1.25	±1.25	±1.25	±1.25
y (m)	-25	-20	-15	-10	-5	0
z (m)	0.5	0.5	0.5	0.5	0.5	0.5
	S07	S08	S09	S10	S11	
x (m)	±1.25	±1.25	±1.25	±1.25	±1.25	
y (m)	5	10	15	20	25	
z (m)	0.5	0.5	0.5	0.5	0.5	
	R00	R01	R02	R03	R04	Rout
x (m)	±5	±5	±5	±5	±5	±5
y (m)	0	0	0	0	0	0
z (m)	1.225	6.55	9.55	12.55	15.55	1.2

3.2 Green covers scenarios

The scenarios consist in modifying the absorbing properties of the frontages and/or of the rooftops for one or both buildings. The differences between scenarios concern the floors 1 to 4 of the buildings and their rooftops. In order to identify them, the following notations will be adopted. Each scenario name is made up of a set of sequences separated by hyphens which begin with a building part (R and F standing for Rooftops and building facades Floors respectively) followed by the side of the street (L for left and R for right) and, for floors only, by a number concerning the floors (1-4 designates the floors 1 to 4 whereas 1-2 and 3-4 concern only the two corresponding floors). Each sequence is ended by _0 or _100 standing for 0% of vegetation (*i.e.* perfectly reflecting surface) or 100% respectively. As the material properties of the computational domain boundaries differs strictly at these locations from among scenarios, others boundaries like the first facades floor of the buildings and the ground are considered as perfectly reflecting surfaces.

The surfaces concerned by the modifications are either perfectly reflecting or absorbing, *i.e.* characterized by an impedance boundary condition. An impedance measurement campaign of the acoustic properties of existing vegetation-covered surfaces has ensured to determine the specific airflow resistivity σ in order to introduce realistic parameters for the simulations. The mean values obtained are σ_F=60 kN.s.m^{-4} for the green frontages and σ_R=400 kN.s.m^{-4} for the green rooftops.

[2] http://i-simpa.ifsttar.fr/

4 Results and discussion

The effect of the locations and of the ratio of green cover surfaces is studied in terms of soundscapes indicators such as the sound pressure level (SPL) and the reverberation time (RT). Simulations have first been performed in 2D on the foreground cross-section of a canyon street illustrated at Fig. 4 for each scenario (on a 2 s duration) in order to estimate the impact of the vegetation covers on sound pressure levels for a wide frequency bandwidth. The maximal frequency of calculations validity is 1000 Hz which implies a mesh discretization $\Delta l = 0.05$ m and a time step $\Delta t = 1 \cdot 10^{-4}$ s. Thus the simulation spreads over 19798 time increments and the computational domain is compounded of nearly 4 millions cells. The sources SL06 and SR06 emits the same pulse at $8 \cdot 10^{-3}$ s intervals. Figure5 presents the continuous equivalent SPL (2 s integration) maps obtained for both extreme scenarios, *i.e.* the scenario for which all boundaries are perfectly reflecting (RL_0-RR_0-FL14_0-FR14_0) and the one with vegetal cover at the rooftops and the floors 1 to 4 of each facade (RL_100-RR_100-FL14_100-FR14_100). Qualitatively, the effect of the vegetation cover is relevant with the expected physical phenomena. Quantitatively, the gain observed as a result of the green covering is about 5 dB. The

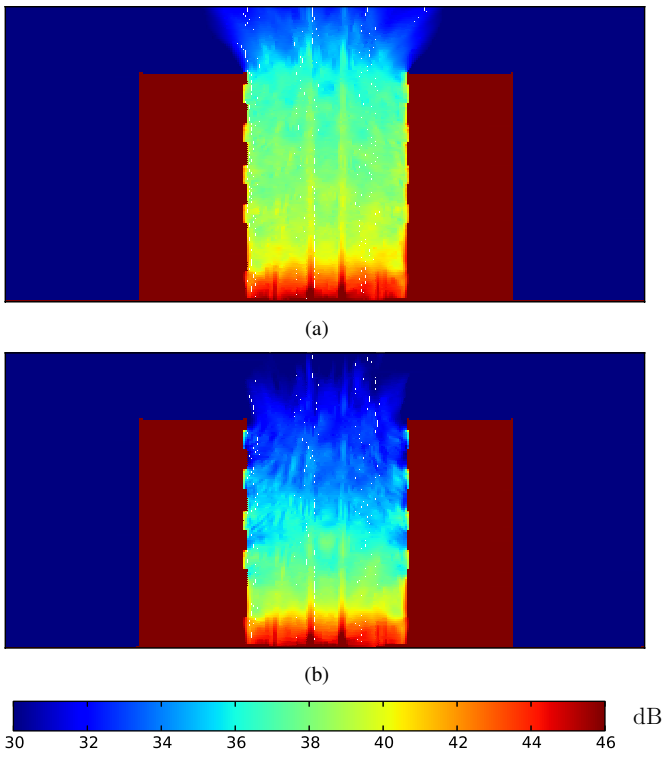

Figure 5: Continuous equivalent sound pressure levels (L_{eq}) maps integrated on a duration of 2 s for (a) the full reflecting scenario (RL_0-RR_0-FL14_0-FR14_0) and (b) the full vegetalized one (RL_100-RR_100-FL14_100-FR14_100).

SPL relative to the reference scenario (RL_0-RR_0-FL14_0-FR14_0) are presented at Fig.6 for each third-octave bands for the microphone RLout located out of the street near the left-side building (*see* Fig. 4). Two groups can be easily distinguished according to the rooftops nature. In addition, it seems that the green covering of the last floors (3 and 4) of the buildings has a more significant effect on sound levels outside the noisy street than vegetalizing the lower floors (1 and 2). More generally, it is verified qualitatively that the

spectra trends can be related with the distribution of green cover on the building facades as, for each location of vegetation, a particular tendency is observed. On the other hand, green rooftops do not modify drastically interference phenomena but contribute strongly to diminish the global sound level.

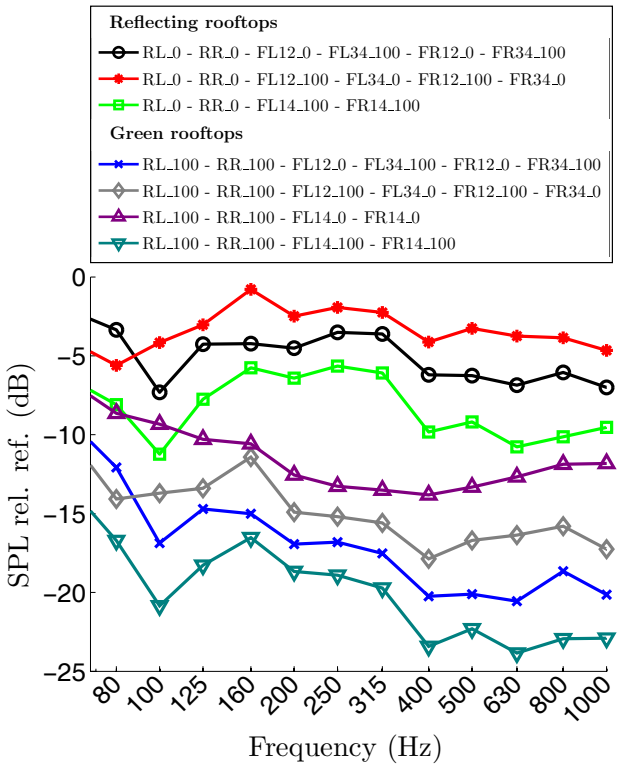

Figure 6: SPL spectra (1/3-octave bands) relative to the reference scenario at microphone RLout.

Sound decreases as reverberation time (RT) can not be rigorously estimated through 2D calculations. Thus simulations have been realized in 3D at lower frequencies with a maximal frequency of validity of 350 Hz in order to limit the computational burden until the 315 Hz 1/3-octave band. The computational domain is still made up of more than 506 millions nodes. The spatial and time steps are $\Delta l = 0.15$ m and $\Delta t = 2 \cdot 10^{-4}$ s respectively. The modelling of incoherent line sources is performed by starting randomly the sources emission at around $1 \cdot 10^{-2}$ s intervals. Fig. 7 gives an example of RT calculating for a sound decrease of 20 dB (RT20)results at microphones RR00, RR03 and RRout. The vegetation has a direct impact on the sound decrease at the bottom of the street when the first floors are covered (Fig. 7(a)). Higher, at third floor, a green cover on the upper floors also tends globally to decrease RT in comparison with the treatment of lower floors (Fig. 7(b)). Although it is not as clear as for the SPL, the observations expressed for the microphone located outside the street (RLout) regarding the location of the vegetation on the facades inside the street are more or less borne out. On the other hand, the rooftop cover has obviously no effect on the RT, neither for the receivers inside the street nor the ones in the shielding area (Fig. 7(c)).

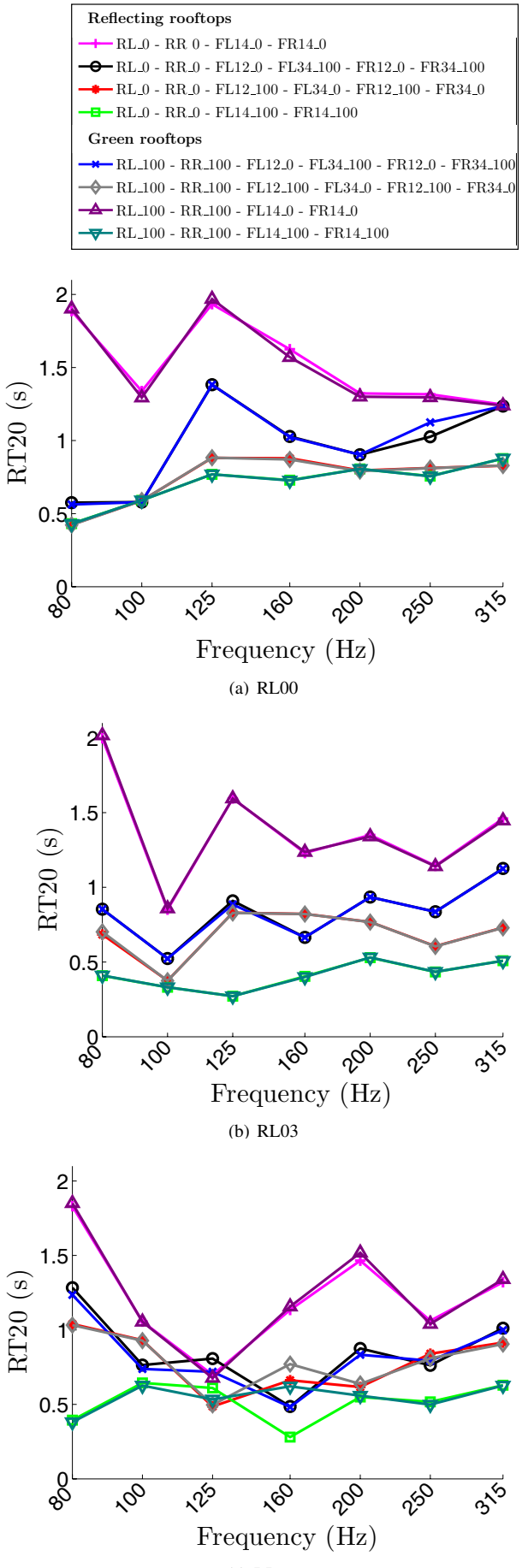

(a) RL00

(b) RL03

(c) RLout

Figure 7: RT spectra (1/3-octave bands) at microphones (a) RL00, (b) RL03 and (c) RLout.

5 Conclusion

An efficient implementation of the TLM method is presented. The OpenCL algorithm takes fully advantage of any

system resources. A voxelization algorithm has also been designed in order to make use of available computer-aided design softwares for creating the input domain of the propagation model. In addition, the computational domain is subdivided in order to allow performing calculations for huge computational domains. The algorithm is applied for evaluating the impact of green cover on urban soundscapes indicators within the framework of the VegDUD project. The effect of the location and of the ratio of vegetation cover on SPL and RT is fairly evident. An interesting point concerns the vegetation cover of the rooftops which decreases the sound pressure level in the shielding area, but does not have any impact on the sound decrease. In this paper, the direct effect of vegetation cover in term of absorption only is studied. However, the modification of the buildings surfaces properties must have an impact on the vertical wind and temperature profiles that could themselves be reflected in the sound propagation in the street. This indirect effect should also be furthermore considered.

Acknowledgments

This work was supported by the french research agency (ANR) in the framework of the VegDUD project (2010-2013) and by the Regional council of the Pays de La Loire (France) within the EM2PAU project (2008-2012).

References

[1] S.-P. Simonaho, T. Lähivaara, T. Huttunen, Modeling of acoustic wave propagation in time-domain using the discontinuous Galerkin method - A comparison with measurements, *Applied Acoustics* **73** (2) (2012) 173–183.

[2] D. K. Wilson, E. L. Andreas, J. W. Weatherly, C. L. Pettit, E. G. Patton, P. P. Sullivan, Characterization of uncertainty in outdoor sound propagation predictions, *J. Acoust. Soc. Am.* **121** (5) (2007) 177–183.

[3] B. Cotté, P. Blanc-Benon, C. Bogey, F. Poisson, Time-domain impedance boundary conditions for simulations of outdoor sound propagation, *American Institute of Aeronautics and Astronautics (AIAA) Journal* **47** (10) (2009) 2391–2403.

[4] D. Luebke, G. Humphreys, How GPUs Work, *Computer* **40** (2) (2007) 96–100.

[5] N. Röber, U. Kaminski, M. Masuch, Ray acoustics using computer graphics technology, in: *Tenth International Conference on Digital Audio Effects* (DAFx-07), Bordeaux, France, 2007, pp. 10–15.

[6] M. Rumpf, R. Strzodka, Using Graphics Cards for Quantized FEM Computations, in: *IASTED Visualization, Imaging and Image Processing Conference*, 2001, pp. 193–202.

[7] T. Takahashi, T. Hamada, GPU-accelerated boundary element method for Helmholtz' equation in three dimensions, *Int. J. Numer. Methods Eng.* **80** (10) (2009) 1295–1321.

[8] P. Micikevicius, 3D finite difference computation on GPUs using CUDA, in: *Proceedings of 2nd Workshop on General Purpose Processing on Graphics Processing Units*, GPGPU-2, ACM, New York, NY, USA, 2009, pp. 79–84.

[9] C. Obrechta, F. Kuznik, B. Tourancheau, J.-J. Roux, Multi-GPU implementation of the lattice Boltzmann method, *Comput. Math. Appl.* (2011) in Press

[10] M. Schönherr, K. Kucher, M. Geier, M. Stiebler, S. Freudiger, M. Krafczyk, Multi-thread implementations of the lattice Boltzmann method on non-uniform grids for CPUs and GPUs, *Comput. Math. Appl.* **61** (2) (2011) 3730–3743, mesoscopic Methods for Engineering and Science - Proceedings of ICMMES-09.

[11] R. Mehra, N. Raghuvanshi, L. Savioja, M. Lin, D. Manocha, An efficient GPU-based time domain solver for the acoustic wave equation, *Applied Acoustics* **73** (2012) 83–94.

[12] G. Dutilleux, J. Waechter, The TLM method for acoustics: local and distributed implementations in Scilab, *SCILAB 2004 Conference* - Rocquencourt (France).

[13] F. Rossi, Graphics hardware accelerated transmission line matrix procedures, *Ph.D. thesis, Faculty of Electrical and Computer Engineering*, University of Victoria (2008).

[14] G. Dutilleux, Applicability of TLM to wind turbine noise prediction, in: *Second International Meeting on Wind Turbine Noise*, Lyon, France, 2007.

[15] P. Aumond, Numerical modelling for environmental acoustics: simulation of meteorological fields and integration in a propagation model (Modélisation numérique pour l'acoustique environnementale : simulation de champs météorologiques et intégration dans un modèle de propagation), *Ph.D. thesis, Doctoral School SPIGA Science Engineering, Geosciences, Architecture*, Nantes, France (December 2011).

[16] G. Guillaume, J. Picaut, G. Dutilleux, B. Gauvreau, Time-domain impedance formulation for transmission line matrix modelling of outdoor sound propagation, *J. Sound Vib.* **330** (26) (2011) 6467–6481.

[17] Y. Miki, Acoustical properties of porous materials - Modifications of Delany-Bazley models, J. Acoust. Soc. Jap. 11 (1) (1990) 19–24.

[18] B. Cotté, Propagation acoustique en milieu extérieur complexe : problèmes spécifiques au ferroviaire dans le contexte des trains à grande vitesse (Outdoor sound propagation in complex environments: Specific problems in the context of high speed trains), *Ph.D. Thesis, Laboratoire de Mécanique des Fluides et d'Acoustique*, UMR CNRS 5509, École Centrale de Lyon (2008).

[19] G. Guillaume, J. Picaut, G. Dutilleux, B. Gauvreau, Implementation of complex impedance conditions and absorbing layers into a transmission line matrix model for urban acoustics applications, in: *Euronoise*, Edinburgh, Scotland, 2009.